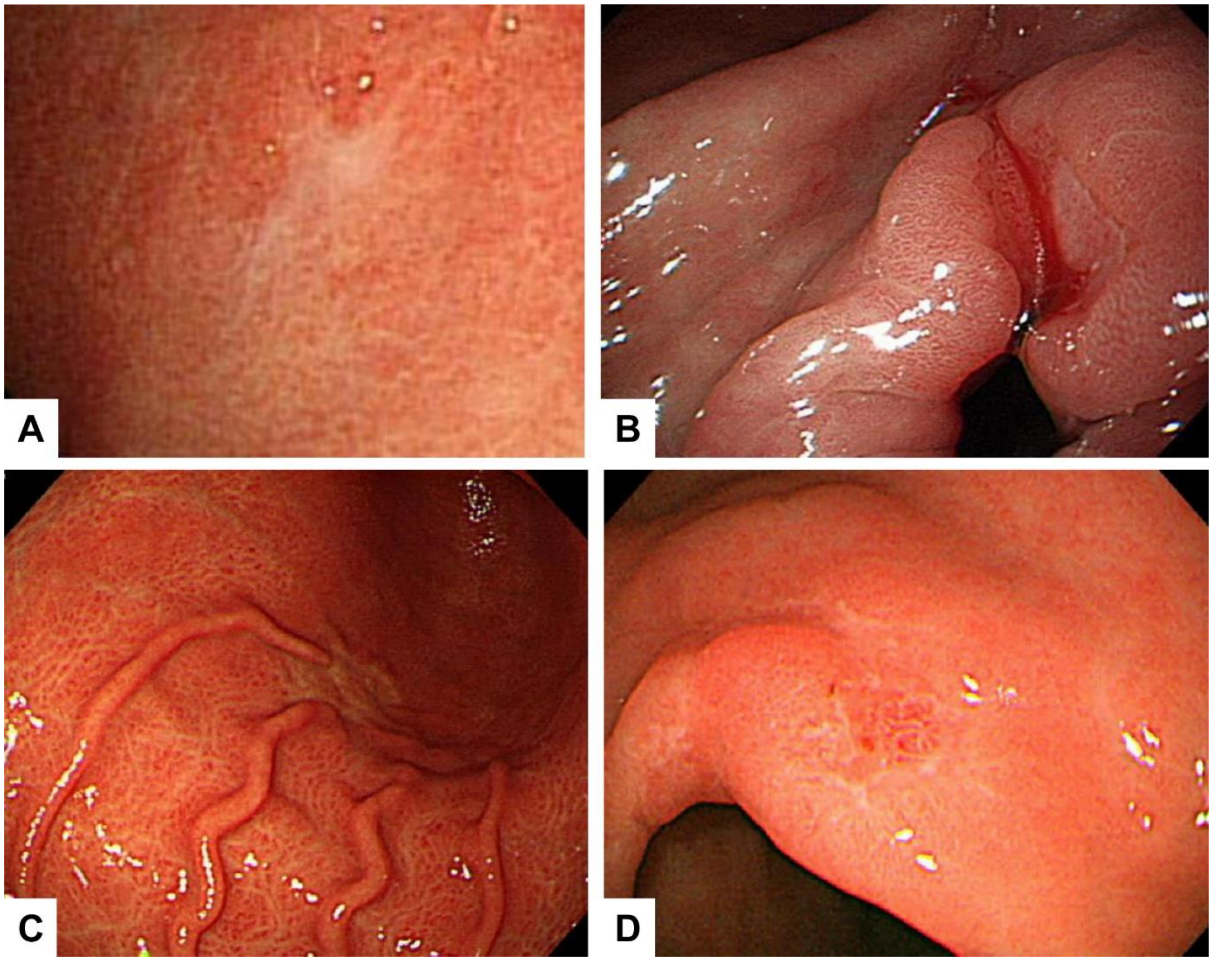

Supplementary Figure 1 Representative images of the endoscopic factors. A: Exudate, B: Endoscopic ulcer, C: Converging fold, D: Tumor island.

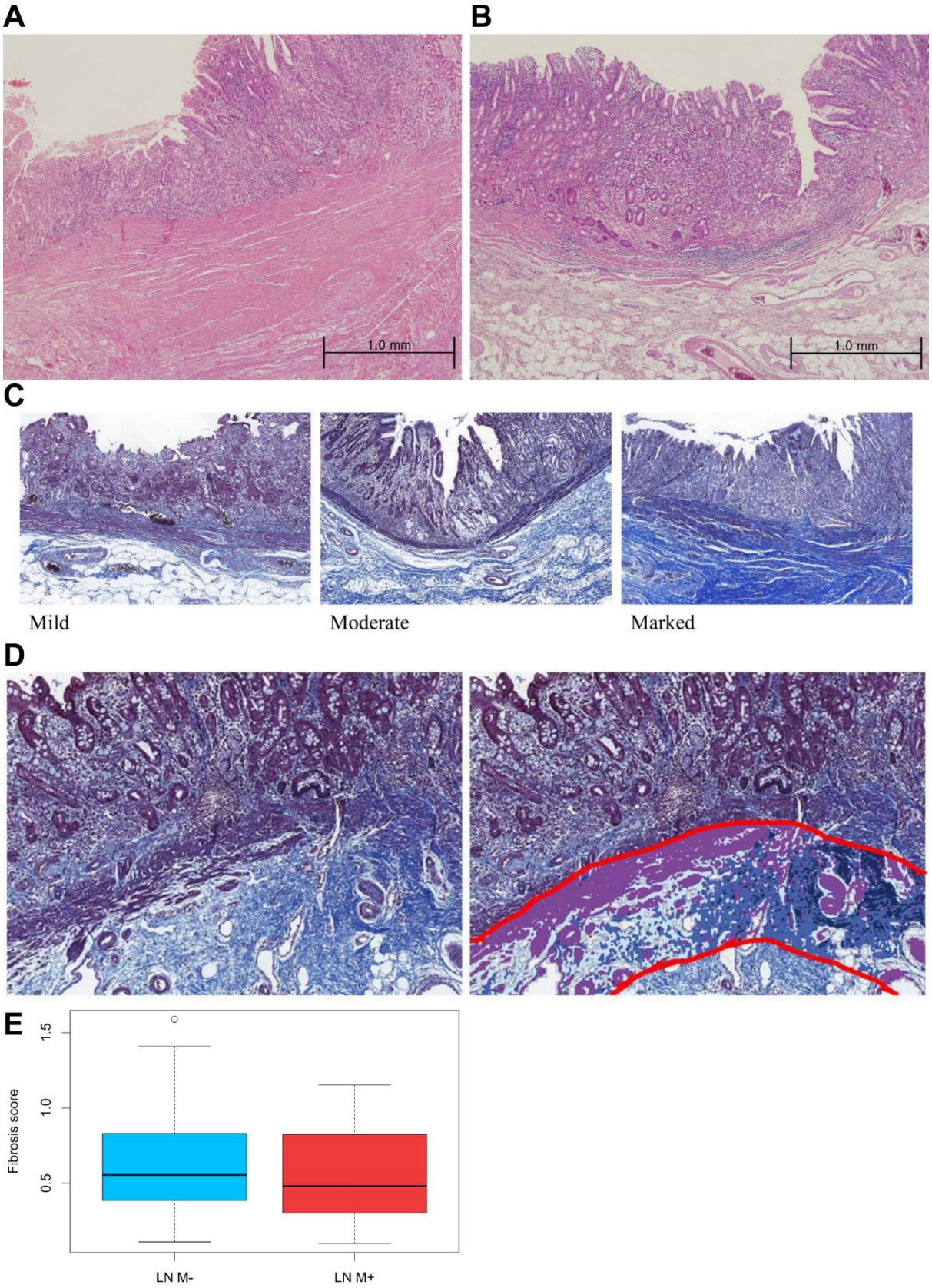

Supplementary Figure 2 Assessment of peritumoral fibrosis. A: Representative

Hematoxylin and eosin (HE) image of tumors with prominent peritumoral fibrosis at 40× magnification; B: Representative HE image of tumors with no fibrosis at 40× magnification; C: Visual assessment of the degree of fibrosis. Representative Masson's trichorome stained microscopic images of mild, moderate, and marked fibrosis are presented; D: Computational analysis of peritumoral fibrosis. Scanned image (left) was opened in QuPath, and the interface between muscularis mucosa and submucosa underneath the tumor was manually annotated (right, red line). Pixel classification was used to discard the empty area (white) and classify the non-empty areas into non-fibrotic (magenta) and fibrotic (blue) areas. The degree of fibrosis (mild, moderate, and marked) is reflected as the brightness of the color; E: Box plot for the fibrosis score (computationally derived metric for the degree and extent of fibrosis) of the Lymph node metasis - and lymph node + groups. LN M-: lymph node metasis negative; LN M+: lymph node metastasis positive.

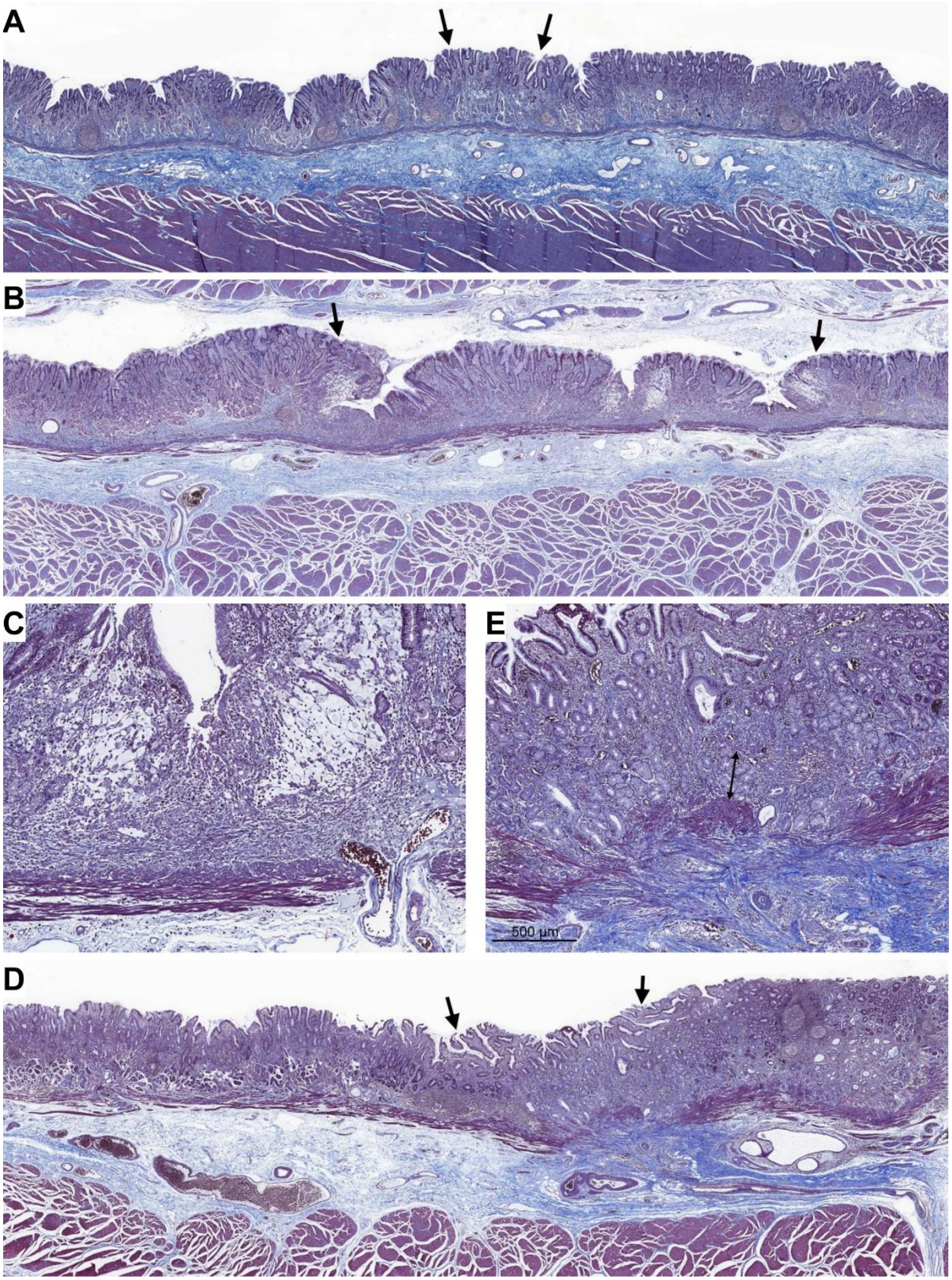

Supplementary Figure 3 Various patterns of muscularis mucosa blurring. A: Absence of blurring in a tumor with substantial peritumoral fibrosis. At the scanning

magnification, muscularis mucosa (MM) underneath tumorous epithelium (both ends marked by arrows) was indistinguishable from that of adjacent MM underneath the non-tumorous epithelium; B: Absence of blurring in a tumor invading the MM. At scanning magnification, the integrity of the MM underneath the tumorous epithelium (both ends marked by arrows) was not noticeably different from that of adjacent MM underneath the non-tumorous epithelium; C: At higher magnification (100×) of (B), tumor cells infiltrating the MM were observed along almost the entire length of the tumor; D: Diffuse blurring of MM in a tumor limited to the lamina propria. At scanning magnification, the blurring of MM was marked enough to readily localize the tumor (both ends marked by arrows); E: At higher magnification (100×) of (D), there were intervening non-neoplastic glands between the deepest tumor cells and MM (marked by a double-headed arrow).

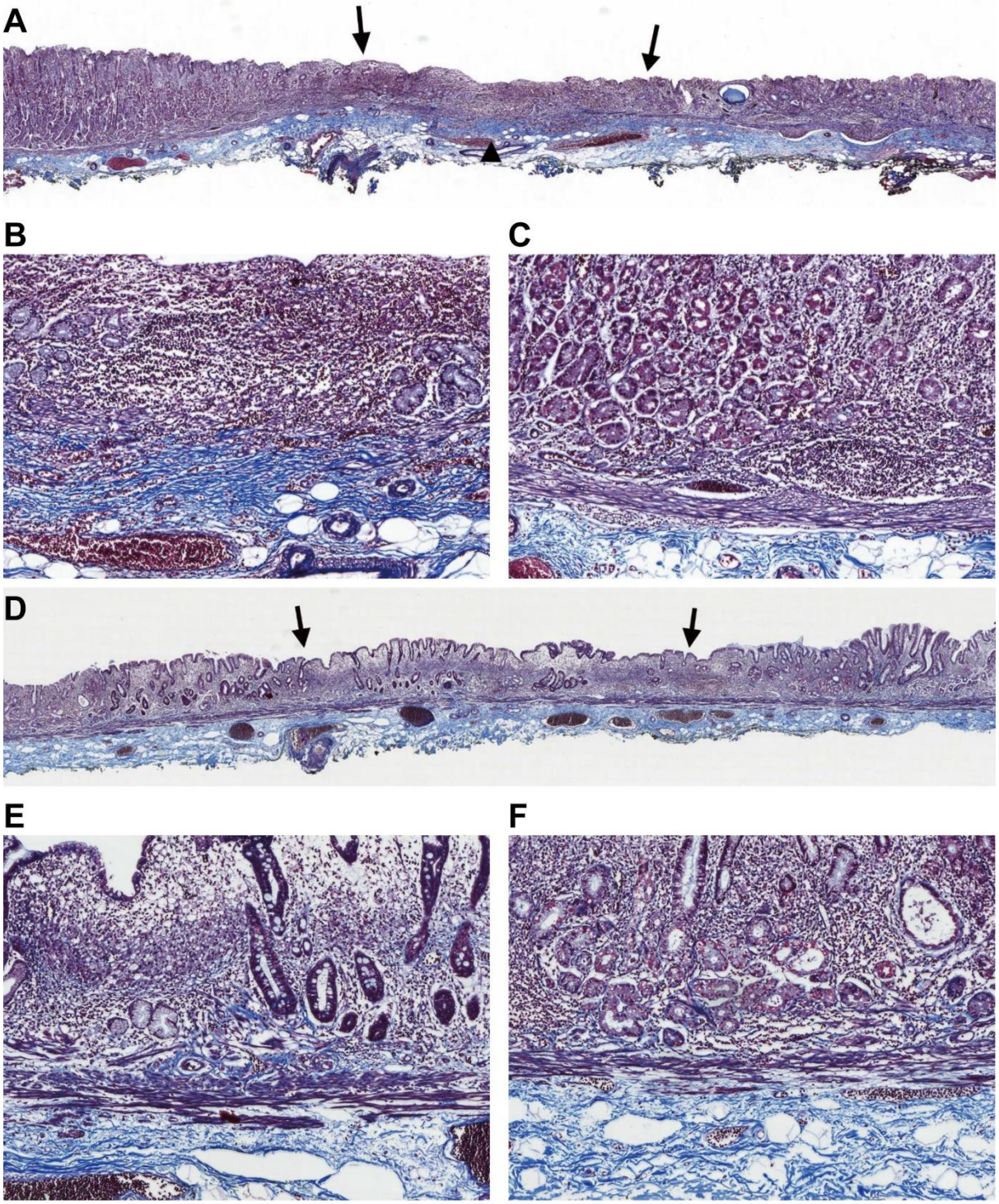

Supplementary Figure 4 Evaluation of muscularis mucosa blurring in endoscpic submucosal dissection specimens. A: Representative Masson's trichrome (MT)-stained image of tumors with muscularis mucosa (MM) blurring at scanning magnification, where both ends of tumorous epithelium are marked by arrows. Note

the disruption of MM at the foci of MM blurring (marked by arrowhead); B: The foci of MM disruption of (A) at higher magnification (200×); C: The intact MM underneath non-tumorous epithelium of A at higher magnification (200×); D: Representative MT-stained image of tumors without MM blurring at scanning magnification. Note that MM underneath tumorous epithelium (both ends marked by arrows) is indistinguishable from that of adjacent MM underneath the non-tumorous epithelium; E: MM underneath tumorous epithelium of (D) at higher magnification (200×); F: MM underneath adjacent non-tumorous epithelium of (D) at higher magnification (200×).

Supplementary Table 1 Histopathologic features associated with blurring of muscularis mucosa

Features	Blurring of MM		*P* value
	Non-diffuse (*n* = 56)	Diffuse (*n* = 29)	
Depth of invasion			< 0.001
LP	48 (85.7)	15 (51.7)	
MM	8 (14.3)	14 (48.3)	
Distance to MM, μm	41 (0–91)	0 (0–18)	< 0.001
Size, cm	1.5 (1.2–1.7)	1.5 (1.2–1.8)	0.314
% of signet ring cells (SRCs)	30 (13.8–70)	30 (0–40)	0.277
Diagnostic category according to the percentage of SRCs			0.140
SRCC	5 (8.9)	3 (10.3)	
PD with SRC component	43 (76.8)	17 (58.6)	
PD	8 (14.3)	9 (31.0)	
Background stomach			0.766
Mild CG	5 (8.9)	3 (10.3)	
Moderate CG or IM	16 (28.6)	11 (37.9)	
CAG	16 (28.6)	8 (27.6)	
CAG with visible *H. pylori*	19 (33.9)	7 (24.1)	
H. pylori abundance			
0	15 (26.8)	10 (34.5)	0.642
1+	13 (23.2)	4 (13.8)	
2+	12 (21.4)	8 (27.6)	
3+	16 (28.6)	7 (24.1)	
TIL abundance			
< 10%	23 (41.1)	9 (31.0)	0.458
10%-20%	25 (44.6)	13 (44.8)	

≥ 20%	8 (14.3)	7 (24.1)	
TP53 expression, n/N			
Loss (0)	2/54 (3.7)	1/28 (3.6)	> 0.999
Wildtype pattern (1+/2+)	49/54 (90.7)	25/28 (89.3)	
Overexpression (3+)	3/54 (5.6)	2/28 (7.1)	
Fibrosis score	0.44 (0.32–0.65)	0.75 (0.62–0.99)	< 0.001

MM: Muscularis mucosa; LP: Lamina propria; SRC: Signet ring cell; SRCC: Signet ring cell carcinoma; PD: Poorly differentiated carcinoma encompassing adenocarcinoma and non-signet ring cell type of poorly cohesive carcinoma; CG: Chronic gastritis; IM: Intestinal metaplasia; CAG: Chronic active gastritis; TIL: Tumor-infiltrating lymphocytes.

Supplementary Table 2 Interobserver reproducibility of muscularis mucosa blurring

	Pathologist 2, *n*	
	Non-diffuse	**Diffuse**
Pathologist 1, *n*		
Non-diffuse	54	2
Diffuse	2	27